0026-895X/00/020409-09$3.00/0

MOLECULAR PHARMACOLOGY, **57:**409–417 (2000).

Huprine X is a Novel High-Affinity Inhibitor of Acetylcholinesterase That Is of Interest for Treatment of Alzheimer's Disease

PELAYO CAMPS, BERNADETTE CUSACK, WILLIAM D. MALLENDER, RACHID EL ACHAB, JORDI MORRAL, DIEGO MUÑOZ-TORRERO, and TERRONE L. ROSENBERRY

Department of Pharmacology, Mayo Foundation for Medical Education and Research and the Department of Research, Mayo Clinic Jacksonville, Jacksonville, Florida (B.C., W.D.M., T.L.R.); and Laboratori de Química Farmacèutica, Facultat de Farmàcia, Universitat de Barcelona, Barcelona, Spain (P.C., R.E.A., J.M., D.M.-T.)

Received August 23, 1999; accepted November 3, 1999

This paper is available online at http://www.molpharm.org

ABSTRACT

Inhibitors of the enzyme acetylcholinesterase (AChE) slow and sometimes reverse the cognitive decline experienced by individuals with Alzheimer's disease. Huperzine A, a natural product used in traditional Chinese herbal medicine, and tacrine (Cognex) are among the potent AChE inhibitors used in this treatment, but the search for more selective inhibitors continues. We report herein the synthesis and characterization of (−)-12-amino-3-chloro-9-ethyl-6,7,10,11-tetrahydro-7,11-methanocycloocta[*b*]quinoline hydrochloride (huprine X), a hybrid that combines the carbobicyclic substructure of huperzine A with the 4-aminoquinoline substructure of tacrine. Huprine X inhibited human AChE with an inhibition constant K_i of 26 pM, indicating that it binds to this enzyme with one of the highest affinities yet reported. Under equivalent assay conditions, this affinity was 180 times that of huperzine A, 1200 times that of tacrine, and 40 times that of E2020 (donepezil, Aricept), the most selective AChE inhibitor currently approved for therapeutic use. The association and dissociation rate constants for huprine X with AChE were determined, and the location of its binding site on the enzyme was probed in competition studies with the peripheral site inhibitor propidium and the acylation site inhibitor edrophonium. Huprine X showed no detectable affinity for the edrophonium-AChE complex. In contrast, huprine X did form a ternary complex with propidium and AChE, although its affinity for the free enzyme was found to be 17 times its affinity for the propidium-AChE complex. These data indicated that huprine X binds to the enzyme acylation site in the active site gorge but interferes slightly with the binding of peripheral site ligands.

Alzheimer's disease is associated with a selective loss of cholinergic neurons in the brain (Davies and Maloney, 1976; Whitehouse et al., 1981). The losses are accompanied by decreases in the neurotransmitter acetylcholine as well as in the respective enzymes that synthesize and degrade acetylcholine, choline acetyltransferase and acetylcholinesterase (AChE) (Perry et al., 1977; Bowen et al., 1982). These observations stimulated a cholinergic hypothesis of Alzheimer's disease (Bartus et al., 1982), which postulates that at least some of the cognitive decline experienced by patients with the disease results from a deficiency in acetylcholine and thus in cholinergic neurotransmission. This hypothesis suggested that inhibitors of AChE might elevate levels of acetylcholine in the brains of these patients and reverse the cognitive decline (Muramoto et al., 1979), and experimental evidence has supported this suggestion. The first, and thus far the only, two drugs approved by the U.S. Food and Drug Administration (FDA) for treatment of the cognitive deficit in Alzheimer's disease are both reversible inhibitors of AChE (Fig. 1). Tacrine (Cognex) was approved in 1993 and E2020 (donepezil, Aricept) in 1996. A third potent reversible AChE inhibitor, huperzine A (Fig. 1), is a natural product isolated from the club moss Lycopodium *Huperzia serrata* used in traditional Chinese herbal medicine (Kozikowski et al., 1992).

A number of efforts have been undertaken to synthesize

This work was supported by Grant NS-16577 from the National Institutes of Health, DAMD 17-98-2-8019 from the U.S. Army Medical Research Acquisition Activity, and by grants from the Muscular Dystrophy Association of America. Financial support from the Comisión Interministerial de Ciencia y Tecnología (Programa Nacional de Tecnología de los Procesos Químicos, Project QUI96–0828), Fundació "La Marató de TV3" (Project 3004/97), Comissionat per a Universitats i Recerca of the Generalitat de Catalunya (Project 1997-SGR-00140), and Medichem, S.A., and fellowships from Comissió Interdepartamental de Recerca i Innovació Tecnològica of the Generalitat de Catalunya to J. Morral and from Agencia Española de Cooperación Internacional (Instituto de Cooperación con el Mundo Arabe, Mediterráneo y Países en Desarrollo) to R.E.A. are gratefully acknowledged.

ABBREVIATIONS: AChE, acetylcholinesterase; MPLC, medium-pressure liquid chromatography; DTNB, 5,5′-dithiobis-(2-nitrobenzoic acid); TcAChE, *Torpedo californica* acetylcholinesterase; TMTFA, *m*-(*N, N,N* trimethylammonio)trifluoroacetophenone; COSY, correlation spectroscopy; HMQC, heteronuclear multiple-quantum coherence.

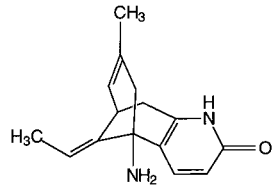

(-)-Huperzine A

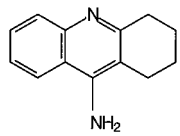

Tacrine

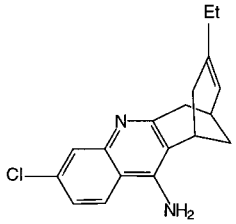

Huprine X

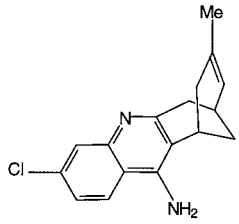

Huprine Y

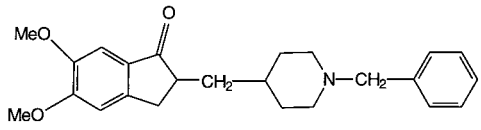

E2020

Fig. 1. Structures of inhibitors of AChE.

even more selective AChE inhibitors as potential therapeutic agents in Alzheimer's disease. Although the highest affinity reversible AChE inhibitors identified to date contain quaternary amine group(s), these efforts have focused on compounds which, like the approved drugs, contain nonquaternary amines and are more likely to pass from the circulation to the brain across the blood-brain barrier. Some new inhibitors have been modeled on tacrine, including bifunctional or bis-tacrine analogs with alkylene linked tacrine moieties (Pang et al., 1996). Other inhibitors have been designed that combine the carbobicyclic substructure of huperzine A with the 4-aminoquinoline substructure of tacrine (Badia et al., 1998). These initial tacrine-huperzine A hybrids, for which we suggest the name huprines, had slightly higher affinity for AChE than tacrine itself. Herein, we introduce a huprine with an ethyl group at position 9 and a chlorine atom at position 3. We designate this compound huprine X (Fig. 1) and show that it inhibits AChE by binding to the enzyme with an affinity that is among the highest yet reported for a reversible inhibitor of AChE.

We also estimate the location of huprine X binding in AChE by reference to the structures of AChE and AChE-inhibitor complexes determined by X-ray crystallography. These structures reveal a deep active site gorge with two sites of ligand interaction: a peripheral site at the surface of the enzyme and an acylation site at the base of the gorge where the substrate acyl group is first transferred to residue S200[1] (Sussman et al., 1991; Harel et al., 1993; Bourne et al., 1995; Harel et al., 1995). Certain ligands can bind selectively to either the acylation site or the peripheral site, and ternary complexes can be formed in which ligands are bound to both sites simultaneously (Taylor and Lappi, 1975; Eastman et al., 1995). X-ray crystallography has shown that edrophonium, huperzine A, and tacrine all are specific for the acylation site, although their contacts with the enzyme surface do not completely overlap (Harel et al., 1993; Raves et al., 1997). Ligands specific for the peripheral site include the small aromatic compound propidium. By examining inhibition of AChE by huprine X in the presence of either propidium or edrophonium, we show that huprine X appears to bind to the acylation site of AChE.

Experimental Procedures

Materials

Human erythrocyte AChE (Rosenberry and Scoggin, 1984; Roberts et al., 1987) and recombinant human AChE (Mallender et al., 1999) were purified as outlined previously. Analyses were conducted with human erythrocyte AChE except where noted, and active site AChE concentrations for both enzymes were determined by assuming 410 U/nmol.[2] Recombinant *Drosophila* AChE was the SEC1 variant (Incardona and Rosenberry, 1996). Human butyrylcholinesterase was purified from plasma (Lockridge, 1990) and was a gift from Dr. Oksana Lockridge, University of Nebraska Medical Center. Propidium iodide was obtained from Calbiochem (La Jolla, CA), and propidium concentrations were assigned with an extinction coefficient $\epsilon_{493\ nm} = 5900\ M^{-1}\ cm^{-1}$ (Taylor and Lappi, 1975). Tacrine was purchased from Sigma Chemical Co. (St. Louis, MO) and E2020 was a gift from Yoshiyuki Kawakami, Ph.D., Eisai Co., Ltd., Ibaraki, Japan.

General Chemistry Methods

Melting points were determined in open capillary tubes with a MFB 595010 M Gallenkamp melting point apparatus. ^{1}H NMR spectra were recorded at 500 MHz on a Varian VXR 500 spectrometer and ^{13}C NMR spectra were recorded at 75.4 MHz on a Varian Gemini 300 spectrometer. The chemical shifts are reported in parts per million (δ scale) relative to internal trimethylsilane and coupling constants are reported in Hertz. Correlation spectroscopy (COSY) ^{1}H/^{1}H experiments were performed with standard procedures and COSY ^{1}H/^{13}C experiments with the ^{1}H-detected heteronuclear multiple-quantum coherence (HMQC) sequence and an indirect detection probe. Infrared (IR) spectra were run on a Perkin Elmer model 1600 Fourier transform/infrared spectrometer. Absorption values are expressed as wavenumbers (cm^{-1}). Optical rotations were measured on a Perkin Elmer model 241 polarimeter. Chiral HPLC analyses were performed on a Waters model 600 liquid chromatograph provided with a Waters model 486 variable λ detector, with a CHIRALCEL OD-H column (25 $\times$ 0.46 cm) containing the chiral stationary phase cellulose tris(3,5-dimethylphenylcarbamate). Conditions A: mixture of hexane/EtOH in the ratio of 75:25, containing

[1] Throughout this paper, we number residues according to the TcAChE sequence. For example, W84 and S200 in this sequence correspond to W86 and S203, respectively, in mammalian AChE.

[2] One unit of AChE activity corresponds to 1 μmol of acetylthiocholine hydrolyzed per minute under standard pH-stat assay conditions, and these conditions correspond to maximal AChE activity at pH 8 (Rosenberry and Scoggin, 1984). Our conventional spectrophotometric assay at 412 nm is conducted in pH 7 buffer with 0.5 mM acetylthiocholine, conditions that result in 4.5 $\Delta A_{412\ nm}$/min with 1 nM AChE or ~76% of the maximal activity.

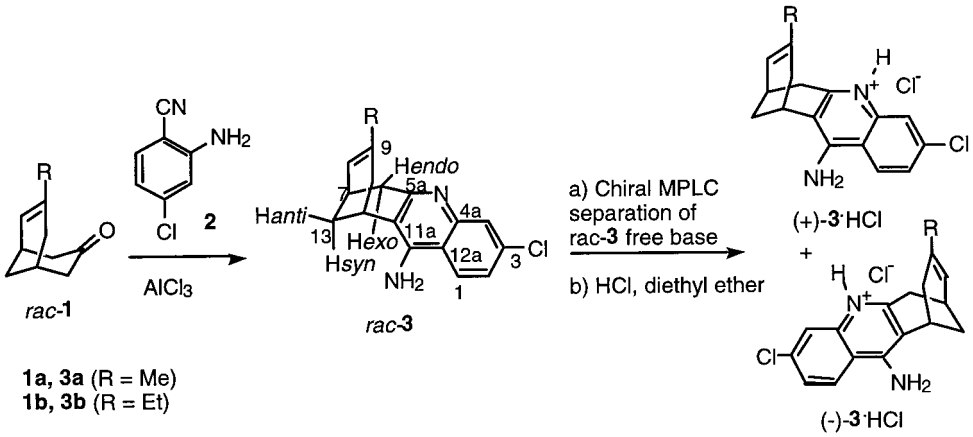

Fig. 2. Synthesis strategy for huprine derivatives. Compound *rac*-**3a** and its enantiomers (huprine Y is the HCl salt of (−)-*rac* **3a**) were prepared as described (Camps et al., 1998, 1999; for the synthesis of related compounds, see Badia et al., 1998). *Rac*-**3b** (huprine X is the HCl salt of (−)-*rac* **3b**) was prepared in a similar way from the known enone *rac*-**1b** (Camps et al., 1996) by Friedländer reaction with 4-chloro-2-aminobenzonitrile, **2** (Camps P, Muñoz-Torrero D, Görbig D, Contreras J, Simon M, Morral J, El Achab R, Badia A, Baños JE, Vivas N. WO patent application 97/13754). Separation of *rac*-**3b** was carried out in a similar manner to that described for *rac*-**3a** (see *Experimental Procedures*). Although the absolute configuration of (−)-**3a** was established by X-ray diffraction analysis, that of (−)-**3b** was assigned by analogy with (−)-**3a** (Camps et al., 1998).

0.1% diethylamine, as eluent, flow 0.20 ml/min, λ = 235 nm. Chiral medium-pressure liquid chromatography (MPLC) separation was carried out on equipment that consisted of a pump (Büchi 688), a variable UV detector (Büchi) and a column (25 × 2.5 cm) containing microcrystalline cellulose triacetate (15–25 μm) as the chiral stationary phase. Column chromatography was performed on silica gel 60 A C.C. (70–200 mesh; SDS, ref. 2100027). For the thin-layer chromatography, aluminum-backed sheets with silica gel 60 F_{254} (Merck; ref. 1.05554) were used. $AlCl_3$ and 2-amino-4-chlorobenzonitrile were purchased from Aldrich Chemical (Milwuakee, WI). Analytical grade solvents were used for recrystallizations, whereas pure for synthesis solvents were used in the reactions and column chromatography. Elemental analyses were carried out at the Mycroanalysis Service of the Centro de Investigación y Desarrollo, C.I.D., Barcelona, Spain.

Synthesis of Huprine X and Huprine Y

The synthesis strategy for these compounds is outlined in Fig. 2.

***rac*-12-Amino-3-chloro-9-ethyl-6,7,10,11-tetrahydro-7,11-methanocycloocta[*b*]quinoline Hydrochloride (*rac*-3b.HCl).** To a suspension of anhydrous $AlCl_3$ (3.00 g, 22.5 mmol) and 2-amino-4-chlorobenzonitrile (2.33 g, 15.3 mmol) in 1,2-dichloroethane (20 ml), a solution of 7-ethylbicyclo[3.3.1]non-6-en-3-one *rac*-**1b** (1.80 g, 11.0 mmol) in 1,2-dichloroethane (115 ml) was added dropwise. The reaction mixture was stirred under reflux for 7 h, allowed to cool to room temperature, diluted with water (80 ml) and tetrahydrofuran (80 ml), made basic by addition of 5 N NaOH, and stirred at room temperature for 30 min. The organic solvents were removed under reduced pressure, and the residue was filtered. The yellowish solid residue (4.20 g) was submitted to column chromatography [silica gel (125 g), hexane/AcOEt, gradient elution]. On elution with hexane/AcOEt 40:60, *rac*-**3b** (1.35 g, 41% yield) was isolated. Subsequent treatment with a solution of HCl (0.37 N solution in MeOH, 3 equiv.), evaporation, and recrystallization of the resulting solid (1.54 g) from MeOH/H_2O 3:10 (26 ml), afforded pure *rac*-**3b**.HCl.2/3H_2O (0.96 g, 25% overall) as a white solid: mp 202–206°C (dec.); IR 3500–2000 (max. at 3333, 3177, 2816, 2671) (CH, NH, and NH^+), 1652, 1634, and 1585 (ar-C-C and ar-C-N) cm^{-1}. ^1H NMR (500 MHz, CD_3OD) δ: 0.89 (t, J = 7.5 Hz, 3 H, CH_2-CH_3), 1.86 (m, 2H, CH_2-CH_3), 1.95 (dm, J = 12.5 Hz, 1 H, 13-H_{syn}), 2.00 (broad d, J = 17.5 Hz, 1 H, 10-H_{endo}), 2.07 (dm, J = 12.5 Hz, 1 H, 13-H_{anti}), 2.53 (broad dd, J = 17.5 Hz, J' = 4.5 Hz, 1 H, 10-H_{exo}), 2.80 (m, 1 H, 7-H), 2.87 (broad d, J = 18.0 Hz, 1 H, 6-H_{endo}), 3.20 (dd, J = 18.0 Hz, J' = 5.5 Hz, 1 H, 6-H_{exo}), 3.38 (m, 1 H, 11-H), 4.82 (s, NH_2 + NH), 5.56 (broad d, J = 5.5 Hz, 1 H, 8-H), 7.56 (dd, J = 9.0 Hz, J' = 1.5 Hz, 1 H, 2-H), 7.75 (d, J = 1.5 Hz, 1 H, 4-H), 8.34 (d, J = 9.0 Hz, 1 H, 1-H). ^{13}C NMR (75.4 MHz, CD_3OD) δ: 12.6 (CH_3, CH_2-CH_3), 27.6 (CH, C11), 28.1 (CH, C7), 29.4 (CH_2, C13), 30.9 (CH_2, CH_2-CH_3), 34.2 (CH_2, C10), 36.1 (CH_2, C6), 115.4 (C) and 115.5 (C) (C11a and C12a), 119.4 (CH, C4), 123.3 (CH, C8), 126.3 (CH, C1), 127.6 (CH, C2), 139.7 (C, C4a), 140.4 (2 C, C3 and C9), 153.2 (C) and 156.6 (C) (C5a and C12). Anal. Calcd. for $C_{18}H_{19}ClN_2$.HCl.2/3H_2O: C, 62.25; H, 6.20; N, 8.07; Cl, 20.42. Found: C, 61.95; H, 6.12; N, 8.08; Cl, 20.44.

Preparative Resolution of *rac*-3b by Chiral MPLC: (+)-(7*R*,11*R*)-3b and (−)-(7*S*,11*S*)-3b (Huprine X). The chromatographic resolution of *rac*-**3b** was carried out with MPLC equipment provided with a column containing microcrystalline cellulose triacetate (15–25 μm), pretreated with a 0.1% solution of Et_3N in ethanol, as the chiral stationary phase. The sample of *rac*-**3b** (1.59 g) was introduced as free base in three portions (1 × 90 mg + 1 × 500 mg + 1 × 1000 mg) with 96% ethanol (2 ml/min) as the sole eluent and solvent. The chromatographic fractions (5 ml) were analyzed by chiral HPLC under conditions A [(−)-**3b**, r.t. 23.87 min, k'_1 = 0.523; (+)-**3b**, r.t. 27.15 min, k'_2 = 0.733; α = 1.40, Res. = 1.75] and combined conveniently. In this way, (−)-**3b** (650 mg, 98% e.e.) and (+)-**3b** (390 mg, 94% e.e.) were obtained. The remaining product consisted of mixtures of both enantiomers with lower e.e. values.

A solution of (−)-**3b** (650 mg) in MeOH (40 ml) was treated with 0.77 N HCl in Et_2O (15 ml). The organic solvents were removed under reduced pressure and the yellowish solid residue (673 mg) was recrystallized from AcOEt/MeOH 3:1 (20 ml) to afford (−)-**3b**.HCl.H_2O {310 mg, $[\alpha]_D^{20}$ = −280 (c = 1.00, MeOH), 99% e.e. by chiral HPLC on the liberated base}: mp 271–273°C (dec.); IR 3500–2500 (max. at 3332, 3171, 2961, 2929, 2818, 2688) (CH, NH, and NH^+), 1651, 1636, and 1587 (ar-C-C and ar-C-N) cm^{-1}. Anal. Calcd. for $C_{18}H_{19}ClN_2$.HCl.H_2O: C, 61.19; H, 6.28; N, 7.93. Found: C, 61.12; H, 6.16; N, 7.80. A pK_a of 8.9 ± 0.1 for (−)-**3b** was determined from relative UV absorbances in sodium phosphate and sodium carbonate buffers (20 mM) at reference wavelengths of 251 and 326 nm and isosbestic points at 256 and 317 nm, respectively.

Similarly, a solution of (+)-**3b** (390 mg) in MeOH (10 ml) was treated with 0.77 N HCl in Et_2O (10 ml). The organic solvents were removed under reduced pressure and the yellowish solid residue (410 mg) was recrystallized from AcOEt/MeOH 3:1 (10 ml) to afford (+)-**3b**.HCl.5/4H_2O {180 mg, $[\alpha]_D^{20}$ = +260 (c = 1.00, MeOH), 97% e.e. by chiral HPLC on the liberated base}: mp 289–291°C (dec.); IR 3500–2500 (max. at 3380, 3186, 2929, 2826, 2683) (CH, NH, and NH^+), 1651, 1635, and 1586 (ar-C-C and ar-C-N) cm^{-1}. Anal. Calcd. for $C_{18}H_{19}ClN_2$.HCl.5/4H_2O: C, 60.42; H, 6.34; N, 7.83. Found: C, 60.40; H, 6.15; N, 7.89.

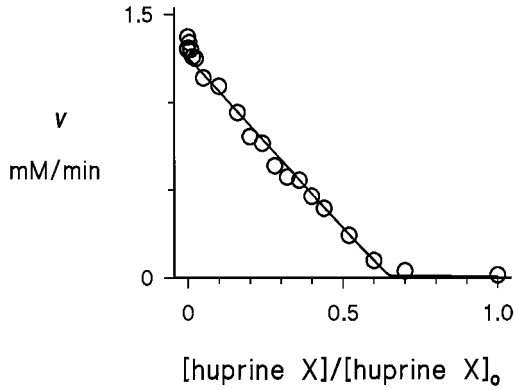

Fig. 3. Titration of recombinant human AChE with huprine X. Each point represents one mixture with a final concentration of 1.21 μM AChE and the indicated concentration of huprine X relative to the maximal concentration [huprine X]$_o$ incubated for 3 h at 23°C. Aliquots (10 μl) were then diluted 300- to 15,000-fold into assay solution containing 0.5 mM acetylthiocholine. Points represent observed v (mM/min) normalized to a 300-fold dilution into assay solution. The line was fitted to the points in a nonequilibrium analysis with the program SCoP, assuming that huprine X interacted with AChE according to Scheme 1 with rate constants $k_I = k_{AI}$ and $k_{-I} = k_{-AI}$ given in Fig. 5. The fitted value of [huprine X]$_o$ = 1.87 μM was used to determine an apparent extinction coefficient for huprine X.

Calibration of Huprine Concentrations by Titration with AChE

AChE active site concentrations can be estimated to an accuracy of better than 10% from the AChE activity assay described below, and stock concentrations of inhibitors can be determined by stoichiometric titration with the enzyme (Eastman et al., 1995; Mallender et al., 1999). Titration of AChE with huprine X gave a linear decrease in AChE activity with increasing concentrations of huprine X (Fig. 3), consistent with the formation of an inactive huprine X-AChE complex. However, the stock concentration of huprine X calculated by assuming 1:1 stoichiometry in this complex was about half of that calculated directly from the dry weight. Because there is no crystallographic or kinetic evidence that a high-affinity inhibitor binds with >1:1 stoichiometry to the AChE active site, we calculated an apparent extinction coefficient of 18 ± 1 mM^{-1} cm^{-1} for huprine X from the absorbance at 326 nm and the concentration determined by the titration in duplicate experiments. This extinction coefficient also was used to estimate concentrations of huprine Y.

Steady-State Inhibition of Enzyme-Catalyzed Substrate Hydrolysis

Inhibitor was preincubated with AChE or butyrylcholinesterase in buffer (20 mM sodium phosphate and 0.02% Triton X-100 at pH 7.0) for 30 min, except for 1 to 6 h preincubations of huprine X and Y with human AChE. Substrate hydrolysis rates v were measured at 25°C after addition of small aliquots of acetylthiocholine and DTNB (to a final concentration of 0.33 mM) in a total volume of 1.0–3.0 ml. Hydrolysis was monitored in an Ellman assay by formation of the thiolate dianion of 5,5′-dithiobis-(2-nitrobenzoic acid) (DTNB) at 412 nm ($\Delta\epsilon_{412\ nm}$ = 14.15 mM^{-1} cm^{-1}; Riddles et al., 1979) for 1 to 3 min on a Varian Cary 3A spectrophotometer (Ellman et al., 1961), and substrate concentrations were corrected for substrate depletion resulting from hydrolysis during this interval. It was assumed that acetylthiocholine concentrations were maintained at low enough values (<1.0 mM) to ignore substrate inhibition in the absence of inhibitors (Szegletes et al., 1999) and that inhibitors that bind exclusively to the acylation site in AChE are unable to form ternary complexes with substrate. These assumptions allow analysis of the inhibition data to be based on Scheme 1.

In Scheme 1, the initial enzyme-substrate complex ***ES*** can form an acyl enzyme intermediate ***EA*** with the rate constant k_2. The inhibitor (**I**) can bind to the free enzyme ***E*** or to ***EA*** with respective

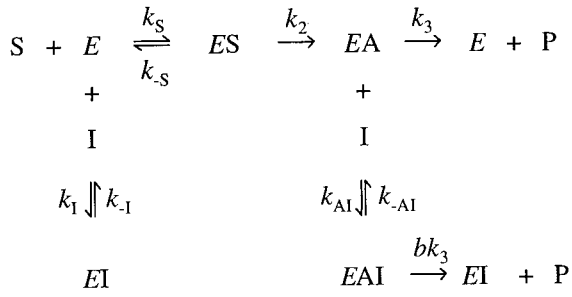

Scheme 1.

equilibrium constants K_I ($=k_{-I}/k_I$) and K_{AI} ($=k_{-AI}/k_{AI}$), and the deacylation rate constant k_3 is altered by a factor b in the ***EAI*** complex. According to Scheme 1, v is given by eq. 1.

$$v^{-1} = \frac{1}{V_{max}}\left[1 + \frac{[I]}{K_U} + \frac{K_{app}}{[S]}\left(1 + \frac{[I]}{K_I}\right)\right] \quad (1)$$

In this equation, V_{max} and K_{app} have been defined previously (Szegletes et al., 1998) and K_U is defined below. Consistent with eq. 1, reciprocal plots of v^{-1} versus $[S]^{-1}$ at all inhibitor (**I**) concentrations were linear with a slope of K_{app}/V_{max} in the absence of inhibitor. Slopes and intercepts of these plots were the respective reciprocals of the second- and first-order rate constants for substrate hydrolysis at a given concentration of **I** and were calculated by a weighted linear regression analysis (Fig. P, version 6.0; Biosoft, Milltown, NJ) that assumed that v has a constant percentage of error. The slopes were normalized by K_{app}/V_{max} as in eq. 2, and values of K_I were determined by linear regression analyses of these normalized slopes versus [I] according to eq. 2, with slope values weighted by the reciprocal of their variance (Eastman et al., 1995).

$$\frac{\text{slope}(v^{-1}\text{ vs }[S]^{-1})}{K_{app}/V_{max}} = \left(1 + \frac{[I]}{K_I}\right) \quad (2)$$

A similar analysis of the intercepts of the reciprocal plots gave K_U in eq. 1, where $K_U = k_3(K_R + b[I])/(k_{cat}(1 - b + (bk_3/k_{-I})))$, $K_R = (k_{-AI} + bk_3)/k_{AI}$, and $k_{cat} = k_2k_3/(k_2 + k_3)$ (Rosenberry, 1975). When the intercepts increase linearly with [I], K_U is a constant that corresponds to k_3K_{AI}/k_{cat} (when $bk_3 \ll k_{-AI}$) or to $k_3k_{-I}/k_{cat}k_{AI}$ (when $k_{-I} \ll bk_3$). For acetylthiocholine hydrolysis by human AChE, k_3 is ~10^4 s^{-1} and k_{cat} is about one-half of k_3 (Szegletes et al., 1999).

When an inhibitor (**I1**) specific to the acylation site is incubated with AChE together with varying concentrations of a second inhibitor (**I2**) specific for the AChE peripheral site, ternary complexes with both inhibitors bound simultaneously to the enzyme can occur (Taylor and Lappi, 1975; Szegletes et al., 1998). At equilibrium, the residual concentration of free enzyme [*E*] in the presence of both inhibitors relative to the concentration of free enzyme $[E]_{[I2]=0}$ when only **I1** is present is given by eq. 3.

$$\frac{[E]}{[E]_{[I2]=0}} = \frac{K_{I2}\left(1 + \frac{[I1]}{K_{I1}}\right)}{K_{I2}\left(1 + \frac{[I1]}{K_{I1}}\right) + [I2]\left(1 + \frac{[I1]}{K_{I12}}\right)} \quad (3)$$

In this equation, K_{I1} is the equilibrium dissociation constant for **I1** with *E*, K_{I2} is the equilibrium dissociation constant for **I2** with *E*, and K_{I12} is the equilibrium dissociation constant for **I1** with the ***EI2*** complex. The concentrations [*E*] and $[E]_{[I2]=0}$ are proportional to the second-order rate constants for substrate hydrolysis noted under eq. 1, and their ratio herein was estimated from the relative v for acetylthiocholine hydrolysis.

Slow Equilibration of an Inhibitor with AChE

Association rate constants were determined from the progressive inhibition of AChE with time as the inhibitor approached equilibrium binding (Eastman et al., 1995; Szegletes et al., 1998). Binding was initiated at 23°C in buffer, in most cases under pseudo first-order conditions in which the concentration of **I** in the incubation mixture was adjusted to at least four times the concentration of AChE. At various times t, a 1.0-ml aliquot was removed to a cuvette, and 40 μl of acetylthiocholine and DTNB was added to a final concentration of 0.5 and 0.33 mM, respectively. The initial hydrolysis rate v was immediately recorded at 412 nm, and the series of v at various t was fitted to eq. 4 by a weighted nonlinear regression analyses (Fig. P), which assumed that v has a constant percentage of error.

$$v = v_{\text{final}} + (v_{\text{initial}} - v_{\text{final}})e^{-kt} \quad (4)$$

In eq. 4, k is the observed pseudo first-order rate constant for the approach to equilibrium, and v_{initial} and v_{final} are the calculated values of v at time zero and at equilibrium, respectively. The dependence of k on [I] was analyzed by weighted linear regression analysis according to eq. 5, with k values weighted by the reciprocal of their variance.

$$k = k_{\text{I}}[\text{I}] + k_{-\text{I}} \quad (5)$$

Equation 5 assumes a simple bimolecular reaction of **I** with AChE, where k_{I} is the association rate constant and $k_{-\text{I}}$ is the dissociation rate constant (Eastman et al., 1995).

In some cases, hydrolysis rates v were fitted directly to a general steady-state solution of Scheme 1 with the program SCoP (version 3.51; Simulation Resources, Inc., Redlands CA) (Szegletes et al., 1998, 1999). This program solves rate equations numerically and allows fitting of v at times before inhibitor equilibrium.

AChE Peripheral Site Binding Affinity Determined by Fluorescence Titration

Binding of propidium to the AChE peripheral site was monitored by enhancement of the propidium fluorescence on a Perkin-Elmer LS-50B luminescence spectrometer in 1 mM sodium phosphate buffer and 0.02% Triton X-100 at 23°C (Taylor and Lappi, 1975). Measurements were performed in a low ionic strength buffer to increase the affinity of propidium (Taylor and Lappi, 1975). Propidium fluorescence was monitored with excitation at 500 nm and emission from 590 to 630 nm. Fluorescence contributions from scatter in the buffer and enzyme were subtracted. Total areas under the fluorescence emission curves (f) were fitted by nonlinear regression analysis (Fig. P) to eq. 6.

$$\text{F} = f_{\text{a}}\text{L}_{\text{tot}} + 0.5(f_{\text{b}} - f_{\text{a}})[\text{D} - \sqrt{\text{D}^2 - 4E_{\text{tot}}\text{L}_{\text{tot}}}\,] \quad (6)$$

In eq. 6, f_{a} is the fluorescence intensity coefficient for free propidium, f_{b} is the fluorescence intensity coefficient for bound propidium, E_{tot} is the total enzyme concentration, L_{tot} is the total propidium concentration, K_{D} is the equilibrium dissociation constant, and $\text{D} = E_{\text{tot}} + \text{L}_{\text{tot}} + K_{\text{D}}$. Estimates of K_{D} are obtained with greatest accuracy from eq. 6 when $\text{L}_{\text{tot}} < K_{\text{D}}$. Data were fitted to eq. 6 with the calculated E_{tot} as the independent variable and L_{tot} at a fixed propidium concentration (0.2 and 2 μM for the binding to AChE and the huprine X-AChE complex, respectively) to give f_{a}, f_{b}, and K_{D}.

Molecular Modeling of Ternary Complex of AChE with Huprine X and Propidium

Construction and analyses of three-dimensional models were performed on a Silicon Graphics workstation Indigo2 IMPACT with QUANTA98 (Molecular Simulations, Inc., Waltham, MA). Modeling of the ternary complex of *Torpedo californica* AChE (TcAChE) with propidium and huprine X began with the crystal structure coordinates for the TcAChE-tacrine complex (Protein Data Bank file: 1ACJ) (Harel et al., 1993). Propidium was manually docked into the peripheral site with the same procedure as described previously (Barak et al., 1994; Szegletes et al., 1998). Huprine X was built from atomic coordinates of 9-methyl huprine (provided by Dr. Javier Luque, Departament de Fisicoquímica, Universitat de Barcelona) and manually docked into the acylation site to maximize the molecular overlap with the aminoquinoline portion of tacrine (Fig. 1). The resulting structure was optimized by energy minimization with CHARMm module of QUANTA98 (conjugate gradient) starting with refinement of the propidium, huprine X and gorge solvent molecules. Subsequent molecular optimization added all amino acid side residues in proximity to the propidium and huprine X ligands.

Results and Discussion

Comparison of Inhibition Constants for Various Inhibitors with AChE. Scheme 1 provides a framework for the analysis of inhibitors that bind to the acylation site of AChE. Steady-state inhibition data for huprine X and two other inhibitors in Fig. 1 is shown in Fig. 4. The reciprocal plots for all three inhibitors (Fig. 4, A–C) show both increasing slopes and increasing intercepts with higher inhibitor concentration. This pattern is often termed "mixed inhibition," and in Scheme 1, it is consistent with significant inhibitor interaction with both the free enzyme E and the acetyl enzyme EA. Replots of the normalized slopes versus the inhibitor concentrations (Fig. 4, D and F) gave estimates of K_{I}, the dissociation constant for inhibitor binding to E, as reported in Table 1. The K_{I} of 26 pM for huprine X indicates that it is one of the highest affinity reversible inhibitors for AChE yet reported. The peptide neurotoxin fasciculin, with a K_{I} for human AChE of ~10 pM under these buffer conditions (Eastman et al., 1995), has a slightly higher affinity. This K_{I} for huprine X was comparable with that for the bisquaternary inhibitor ambenonium (Hodge et al., 1992) and the transition state analog *m*-(*N*,*N*,*N*-trimethylammonio)trifluoroacetophenone (TMTFA) (Szegletes et al., 1998).[3] As shown in Table 1, the affinity of huprine X was 180 times higher than that of huperzine A and 1200 times higher than that of tacrine, the two well known inhibitors of AChE upon which the hybrid structure of huprine X was based. Furthermore, the huprine X affinity was 40 times higher than that of E2020. Huprine Y, the analog of huprine X in which a methyl group replaces the ethyl group at position 9, gave a K_{I} similar to that of huprine X (Table 1). The high affinity of huprine X also was very selective for vertebrate AChE relative to other cholinesterases. K_{I} values for the inhibition of human butyrylcholinesterase and *Drosophila* AChE were 120 ± 12 and 55 ± 10 nM, respectively, more than three orders of magnitude higher than that for human AChE.

The reciprocal plots in Fig. 4A show that intercepts as well as slopes were increased in the presence of huprine X. According to eq. 1, an increase in intercepts occurs when the inhibitor can bind to the acetyl enzyme EA and cause the parameter K_{U} to become significant. It is less straightforward to interpret K_{U} in the context of Scheme 1 than K_{I}, but K_{U} for huprine X with acetylthiocholine as substrate appears approximately equal to $k_{-\text{I}}/k_{\text{AI}}$, a ratio similar to the equilib-

[3] The K_{I} determined for TMTFA (50 pM; Szegletes *et al.,* 1998) was based on the total concentration of TMTFA and its hydrate in solution. Because the hydrate is not an AChE inhibitor but is present in 10^5-fold excess over TMTFA (Nair *et al.,* 1993), the intrinsic equilibrium dissociation constant K_{D} for TMTFA itself with AChE is about 10^{-15} M.

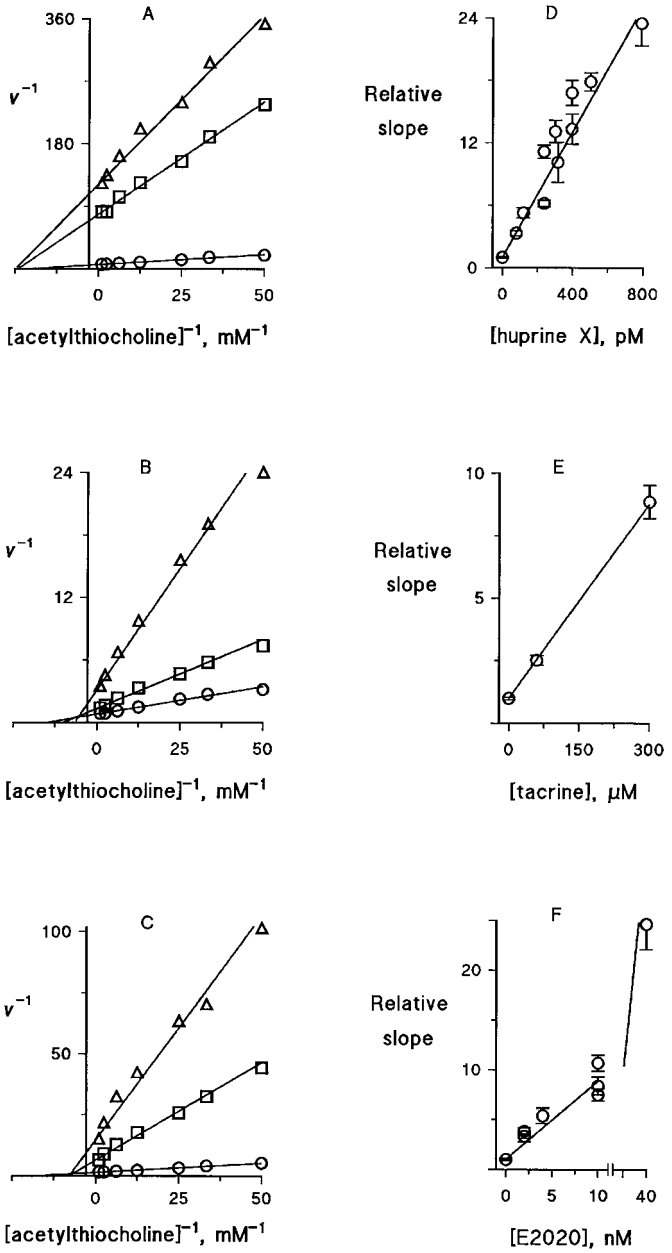

Fig. 4. Steady-state inhibition of AChE hydrolysis of acetylthiocholine. A–C, reciprocal plots of initial velocities ($\Delta A_{412\ nm}$/min) and substrate concentrations were analyzed according to eq. 1. Huprine X concentrations in *A* were 0 (○), 240 (□), and 400 pM (△). Tacrine concentrations in *B* were 0 (○), 60 (□), and 300 nM (△). E2020 concentrations in C were 0 (○), 10 (□), and 40 nM (△). D–F, slopes of plots in A–C were normalized by dividing by the slope in the absence of inhibitor and plotted against the inhibitor concentration according to eq. 2 to derive K_I values (Table 1). Additional points from data not shown in A and C were included in D and F, respectively.

rium constants for the binding of huprine X to *E* and *E*A. This interpretation is based on three conditions outlined in *Experimental Procedures*: The intercepts in Fig. 4A increased linearly with [huprine X] (data not shown); the dissociation rate constant k_{-I} for huprine X was several orders of magnitude smaller than the deacylation rate constant k_3 (see the next section); and k_3 and k_{cat} have similar values (Szegletes et al., 1998). Values of K_U also were obtained for tacrine and E2020 (Table 1), and these values were roughly three times the corresponding K_I values, as has been observed previously for

TABLE 1
Inhibition constants for several inhibitors of AChE.[a]

Inhibitor	K_I	K_U	k_I
	nM	*nM*	$\mu M^{-1}\ min^{-1}$
Tacrine	31 ± 3	104 ± 12	ND
E2020	1.1 ± 0.1	3.6 ± 0.4	ND
Huperzine A	4.6 ± 0.7[b]	ND	5.0 ± 0.2[b]
Huprine X	0.026 ± 0.002	0.024 ± 0.001	440 ± 30
Huprine Y	0.033 ± 0.003	0.038 ± 0.003	400

ND, not determined.
[a] Values of K_I, K_U, and k_I were obtained as outlined in *Experimental Procedures*.
[b] From reference Szegletes et al. (1998) under identical buffer conditions.

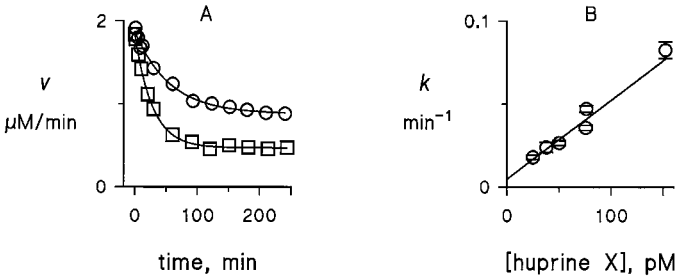

Fig. 5. Association and dissociation rate constants for huprine X and AChE. A, progressive inhibition of AChE (6 pM) with time as huprine X binding approached equilibrium was measured by removing 1-ml aliquots of the reaction mixture and immediately adding DTNB and the substrate acetylthiocholine for assay as outlined in *Experimental Procedures*. Hydrolysis rates v obtained with 25 (○) and 75 (□) pM huprine X were fitted to eq. 4 to obtain a value of k for each curve. B, values of k obtained at several concentrations of huprine X as in A were plotted against [huprine X]. Although the plot was nearly linear, the concentration of huprine X in some cases was not sufficiently in excess of the concentration of AChE to justify analysis with eq. 5. The SCoP fitting program was applied directly to all the association rate data (Szegletes et al., 1998) to obtain k_I = 440 ± 30 $\mu M^{-1}min^{-1}$ and k_{-I} = 0.009 ± 0.003 min^{-1}.

other AChE inhibitors (Rosenberry and Bernhard, 1972). The fact that K_U is comparable with K_I for huprine X and huprine Y arises from the high affinities of these compounds and their consequent slow reequilibration when substrate is added to the assay mixtures. Analysis of v versus time with the program SCoP demonstrated that K_I decreased ~20% and K_U increased by nearly a factor of 2 when v was adjusted for inhibitor equilibration.

Determination of Association and Dissociation Rate Constants for Huprine X and AChE. AChE inhibitors with K_I values in the subnanomolar range often have very low dissociation rate constants that permit measurement of the kinetics of inhibitor association. This was the case with huprine X and huprine Y, as demonstrated in Fig. 5 and Table 1. Rate constants for the approach to equilibrium binding at a fixed concentration of huprine X were estimated as in Fig. 5A, and from the time course of these reactions values of $k_I = 4.4 \pm 0.3 \times 10^8\ M^{-1}min^{-1}$ and $k_{-I} = 0.009 \pm 0.003\ min^{-1}$ were obtained (Fig. 5B). The value of k_I we previously reported for huperzine A in the same buffer (Szegletes et al., 1998) is also shown in Table 1, and this value is only ~1% of the k_I value for either huprine X or huprine Y. In fact, the difference in k_I accounts for almost all of the difference in K_I between huperzine A and the two hybrid compounds, as the k_{-I} values were nearly comparable. However, the k_I value reported herein for huprine X still remained <20% of that previously reported for the bisquaternary AChE inhibitor ambenonium (Hodge et al., 1992) and <1% of that for the

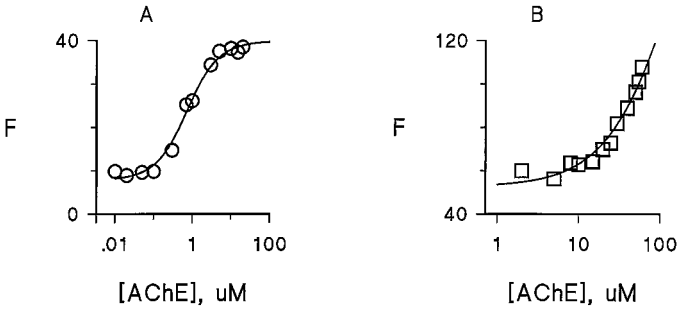

Fig. 6. Fluorescence titration of recombinant human AChE with propidium in the absence (A) and presence (B) of huprine X. A total of three fluorescence spectra was collected and averaged for each AChE titration point as outlined in *Experimental Procedures*, and total areas under the fluorescence emission curves (F) were plotted against the final AChE concentration in the assay sample. A, propidium was added to a total concentration of 0.2 μM to AChE and then successively diluted with a solution of 0.2 μM propidium. The data were fitted to eq. 6 to give f_a = 39 ± 4, f_b = 200 ± 4, and K_D = 0.63 ± 0.10 μM. B, because of the shift in the binding curve for propidium in the presence of huprine X, propidium was added to a higher total concentration of 2 μM to AChE preincubated with 100 μM huprine X and then successively diluted with a solution of 2 μM propidium and 100 μM huprine X. In the presence of huprine X, a plateau in the fluorescence enhancement indicating propidium saturation in the ternary complex was not obtained. However, if the same degree of fluorescence enhancement was assumed for propidium in the ternary complex as in the propidium-AChE binary complex (f_b/f_a = 5.1), the data fitted to eq. 6 gave f_a = 26 ± 1 and K_D = 190 ± 25 μM. This assumption is not necessarily valid, because some disruption of the propidium environment occurs in the presence of huprine X (Fig. 8).

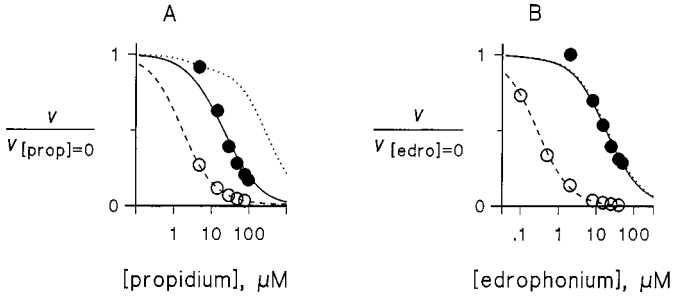

Fig. 7. Determination of the relative affinity of huprine X in the propidium-AChE complex (A) or the edrophonium-AChE complex (B) by inhibition of substrate hydrolysis. AChE (○, 25 pM; ●, 1200 pM) was incubated without (○) or with (●) huprine X (4 nM) and the indicated concentration of propidium or edrophonium for 6 h at 23°C, and a 2.9-ml aliquot was mixed with 100 μl of DTNB and 12 μl of acetylthiocholine to give final concentrations of 0.33 mM DTNB and 20 μM acetylthiocholine. Points represent v observed over a 2- to 5-min interval normalized by the corresponding v obtained at the same [huprine X] in the absence of propidium ($v_{[prop] = 0}$) or edrophonium ($v_{[edro] = 0}$). Lines correspond to normalized v obtained by fitting the experimental data to a complete nonequilibrium reaction scheme with the program SCoP, with kinetic rate constants previously determined for acetylthiocholine and propidium or edrophonium (Eastman et al., 1995; Szegletes et al., 1999) and those in Table 1 for huprine X. The dashed lines correspond to the absence of huprine X and the solid lines, to 4 nM huprine X. The dotted lines correspond to the curves calculated when no ternary complex forms ($1/K_{I12}$ = 0). Based on data with 4 nM huprine X as well as with 1 and 2 nM huprine X (data not shown) with both propidium and edrophonium, the procedure in A gave K_{I2} = 1.4 μM for propidium, K_{I1} = 20 pM for huprine X, and K_{I12}/K_{I1} = 17 ± 3. The procedure in B gave K_{I2} = 0.2 μM for edrophonium, K_{I1} = 29 pM for huprine X, and K_{I12}/K_{I1} > 1000. Lines also were fitted with the much simpler analysis scheme in eq. 3, which required the approximations that v reflects the true second-order rate constant, that the free huprine X concentration remains unchanged through the entire range of propidium or edrophonium concentrations, and that no slow reequilibration occurs in the presence of substrate. Although these approximations held only approximately at best, ratios of K_{I12}/K_{I1} of 12 ± 2 with propidium and >200 with edrophonium were in reasonable agreement with those from the SCoP program.

monoquaternary inhibitor *N*-methylacridinium (Rosenberry et al., 1996). We measured a pK_a of 8.9 for huprine X, indicating that the ring N should be largely protonated at pH 7, so huprine X should be cationic. Thus, the lower k_I for huprine X relative to ambenonium or *N*-methylacridinium appears to indicate some remaining steric or conformational restraints on its rapid association with the AChE active site.

Huprine X Binds to Acylation Site but Slightly Interferes with Binding of Propidium to Peripheral Site. Because crystal structures of AChE show that both tacrine and huperzine A bind to the acylation site (Harel et al., 1993; Raves et al., 1997), we anticipated that huprine X also would bind to the acylation site. To explore this point, we used propidium, a ligand specific for the AChE peripheral site (Taylor and Lappi, 1975). If huprine X binding is confined to the acylation site, a ternary complex of AChE with huprine X and propidium should be able to form. In principle, such a complex can be detected by equilibrium titration or by kinetic analyses. For example, kinetic studies have shown that propidium and huperzine A form a ternary complex with AChE (Szegletes et al., 1998).

We first examined the formation of an equilibrium ternary complex by direct fluorometric measurement of propidium binding to the AChE-huprine X complex. The binding of propidium to the AChE peripheral site results in significant enhancement of propidium fluorescence, a property that has been used to determine the binding affinity of this ligand for the peripheral site (Taylor and Lappi, 1975). Figure 6 illustrates the results of a titration experiment where AChE concentrations were varied in the presence of fixed concentrations of propidium alone or propidium plus huprine X. The 100 μM of huprine X used in this experiment was more than six orders of magnitude higher than the K_I for this compound reported above, ensuring that any detectable propidium binding would have to involve formation of a ternary complex. In the absence of huprine X, the fluorescence of bound propidium was enhanced ~5-fold relative to free ligand (Fig. 6A). A K_D value of 0.63 ± 0.10 μM was obtained, in reasonable agreement with propidium inhibition constants of 0.4 to 1.1 μM obtained previously at a somewhat higher ionic strength (Szegletes et al., 1998). When AChE was saturated with huprine X during the titration, the propidium binding curve was shifted (Fig. 6B). A qualitative increase in propidium fluorescence at higher AChE concentrations was apparent, but values of K_D as well as of the fluorescence intensity coefficient f_b for propidium with huprine X-bound AChE were uncertain. If the fluorescence enhancement for propidium bound to the huprine X-AChE complex was assumed to be the same as that for propidium bound to free AChE, the affinities of propidium and huprine X in the ternary complex decreased about two orders of magnitude relative to those with the free enzyme.

An alternative procedure for measuring the formation of ternary complexes of AChE with huprine X and propidium is to examine the steady-state inhibition of the enzyme in the presence of both inhibitors as illustrated in Fig. 7A. The concentration of huprine X was fixed, and the change in the enzyme activity v as propidium was added to the mixture was analyzed by two methods. One method assumed that the concentration of free AChE [*E*] was given by eq. 3 and was proportional to the substrate hydrolysis rate v at the low

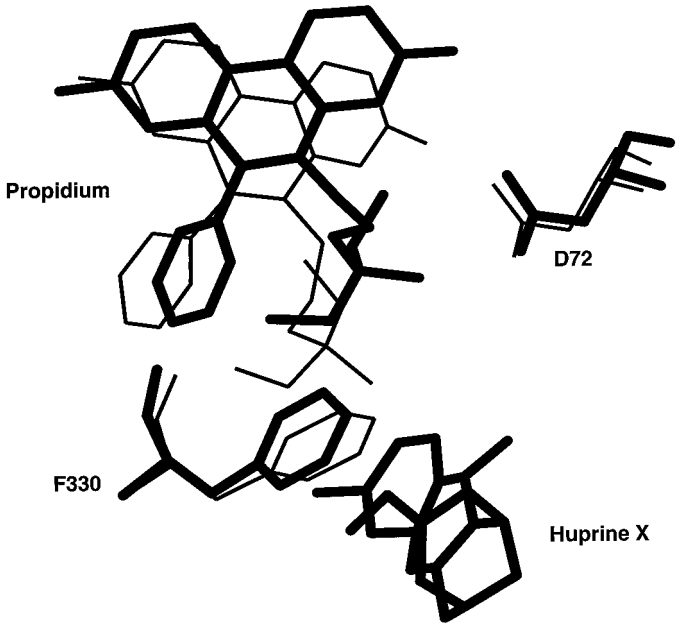

Fig. 8. Molecular modeling of the ternary complex of AChE with huprine X and propidium (see *Experimental Procedures*). AChE ligands and amino acids in the vicinity of the ligands are displayed with all other residues, solvent molecules and water omitted. The thin line indicates the orientations of propidium and amino acids in the propidium-TcAChE complex. The thick line indicates the effect of huprine X in the acylation site on the orientation of propidium, F330, and D72.

substrate concentration (20 μM) used in the assay. The other method avoided these assumptions by fitting v directly in the general steady-state solution with the program SCoP. As indicated in the legend to Fig. 7, the two methods gave reasonable agreement. When huprine X was omitted, increasing concentrations of propidium resulted in the decrease in v indicated by the dashed line and the open symbols in Fig. 7A. If no ternary complex could form, huprine X and propidium would be completely competitive and the decrease in v would correspond to the dotted line in Fig. 7A. Complete competition of huprine X is observed with edrophonium (Fig. 7B), a known acylation site inhibitor (Harel et al., 1993). However, the data for huprine X and propidium fall between the dashed and the dotted lines as indicated by the closed symbols in Fig. 7A, indicating that the ternary complex can form. Fitting this observed data gave an estimate of $K_{I12}/K_{I1} = 17 \pm 3$, indicating that the affinity of huprine X for free AChE was ~17-fold higher than its affinity for the propidium-AChE complex and providing a more accurate measure of the relative affinity than the fluorescence titration above.

Molecular modeling of the ternary complexes of either huperzine A or TMTFA with propidium-TcAChE revealed that the bound propidium does not make close contact with either of these two acylation site inhibitors (Szegletes et al., 1998). In fact, only minimal molecular adjustments were necessary for the propidium molecule to dock into the TcAChE peripheral site in the presence or absence of huperzine A or TMTFA, suggesting little or no interaction between the bound ligands. This was consistent with thermodynamic data showing a reduction of only 5- to 7-fold in the affinity of these ligands in the ternary complex relative to their affinity for free AChE. Most of this reduction could well represent an unfavorable electrostatic interaction between ligands in the ternary complex (Szegletes et al., 1998). Similar modeling of the ternary complex of TcAChE with huprine X and propidium indicated a more unfavorable interaction between the ligands (Fig. 8). Huprine X manually docked within the TcAChE acylation site occupied the position of the aminoquinoline portion of tacrine as observed in the tacrine-TcAChE crystal structure (Harel et al., 1993). This orientation resulted in a high degree of overlap of the carbobicyclic ring portion of huprine X with the position of huperzine A as indicated in the huperzine A-TcAChE crystal structure (Raves et al., 1997). In contrast to the binding of either TMTFA or huperzine A alone, however, insertion of huprine X between F330 and W84 in the acylation site resulted in movement of the F330 side chain away from W84 and up into the gorge toward D72 (Fig. 8). This movement was accompanied by a significant rotation of the phenyl ring of the F330 side chain. As a result of this rearrangement, propidium could not be fit as deeply in the TcAChE peripheral site when huprine X was bound, and portions of the propidium structure were displaced out toward bulk solvent by almost 2Å. Molecular modeling thus supports the experimental data and indicates that although a ternary complex of propidium and huprine X can form with AChE, the binding geometry and added molecular volume of huprine X will result in significant decreases in the affinities of the ligands in the ternary complex.

Other energy minimization analyses of docked huprine-TcAChE complexes result in a very similar huprine X orientation in the AChE active site (Camps et al., 1999). More extensive molecular dynamics calculations also support this orientation (Camps et al., 1999; Barril et al., 1999). Of particular interest are molecular dynamics simulations of the binding of 3-fluoro-9-methyl huprine to TcAChE, which show that the fluorine atom fills a hydrophobic pocket formed by L333, M436, I439, and W432 (Barril et al., 1999). Ligand interactions with this pocket have not been reported previously, and they may account for increases in huprine affinity for AChE of about one order of magnitude in the 3-fluoro and two to three orders of magnitude in the 3-chloro derivatives relative to unsubstituted 9-methyl or 9-ethyl huprines (Camps et al., 1999; present article).

Huprine X May Be Useful in the Treatment of Alzheimer's Disease. The selectivity of an inhibitor of AChE in treating patients with Alzheimer's disease appears to parallel the affinity of the inhibitor for the AChE active site. Thus, E2020, with an affinity some 30 times higher than that of tacrine, is administered at a daily dose of only one-tenth that of tacrine.[4] The lower dosage regimen results in fewer undesirable side effects with E2020 than with tacrine. If this trend is extended by huprine X, which has an AChE affinity yet 40 times higher than that of E2020, huprine X may prove to be an even more attractive drug for the treatment of Alzheimer's disease. Such optimization of the AChE inhibitor of therapeutic choice may provide the most effective treatment until other classes of drugs become available that target the basic cause of Alzheimer's disease.

Acknowledgments

We thank Dr. Javier Luque of the Department de Fisicoquímica, Universitat de Barcelona, for providing atomic coordinates of 9-methyl huprine overlaid on the configuration of AChE-bound ta-

[4] See the Physicians' Desk Reference (1999), Medical Economics Co., Montvale, New Jersey.

crine as well as of a final structure obtained from molecular dynamic simulations of the complex of huprine X with TcAChE.

References

Badia A, Baños JE, Camps P, Contreras J, Görbig DM, Muñoz-Torrero D, Simón M and Vivas NM (1998) Synthesis and evaluation of tacrine-huperzine A hybrids as acetylcholinesterase inhibitors of potential interest for the treatment of Alzheimer's disease. *Bioorg Med Chem* **6:**427–440.

Barak D, Kronman C, Ordentlich A, Ariel N, Bromberg A, Marcus D, Lazar A, Velan B and Shafferman A (1994) Acetylcholinesterase peripheral anionic site degeneracy conferred by amino acid arrays sharing a common core. *J Biol Chem* **269:**6296–6305.

Barril X, Orozco M and Luque FJ (1999) Predicting relative binding free energies of tacrine-huperzine A hybrids as inhibitors of acetylcholinesterase. *J Med Chem* **42:**5110–5119.

Bartus R, Dean R, Beer B and Lippa A (1982) The cholinergic hypothesis of geriatric memory dysfunction. *Science (Wash DC)* **217:**408–417.

Bourne Y, Taylor P and Marchot P (1995) Acetylcholinesterase inhibition by fasciculin: Crystal structure of the complex. *Cell* **83:**503–512.

Bowen DM, Benton JS, Spillane JA, Smith CC and Allen SJ (1982) Choline acetyltransferase activity and histopathology of frontal neocortex from biopsies of demented patients. *J Neurol Sci* **57:**191–202.

Camps P, Contreras J, Font-Bardia M, Morral J, Muñoz-Torrero D and Solans X (1998) Enantioselective synthesis of tacrine-huperzine A hybrids. Preparative chiral MPLC separation of their racemic mixtures and absolute configuration assignments by X-ray diffraction analysis. *Tetrahedron: Asymmetry* **9:**835–849.

Camps P, El Achab R, Font-Bardia M, Görbig D, Morral J, Muñoz-Torrero D, Solans X and Simon M (1996) Easy synthesis of 7-alkylbicyclo[3.3.1]non-6-en-3-ones by silica gel-promoted fragmentation of 3-alkyl-2-oxaadamant-1-yl mesylates. *Tetrahedron* **52:**5867–5880.

Camps P, El Achab R, Görbig DM, Morral J, Muñoz-Torrero D, Badia A, Baños JE, Vivas NM, Barril X, Orozco M and Luque FJ (1999) Synthesis, in vitro pharmacology, and molecular modeling of very potent tacrine-huperzine A hybrids as acetylcholinesterase inhibitors of potential interest for the treatment of Alzheimer's disease. *J Med Chem* **42:**3227–3242.

Davies P and Maloney AJF (1976) Selective loss of central cholinergic neurons in Alzheimer's disease. *Lancet* **2:**1403.

Eastman J, Wilson EJ, Cervenansky C and Rosenberry TL (1995) Fasciculin 2 binds to a peripheral site on acetylcholinesterase and inhibits substrate hydrolysis by slowing a step involving proton transfer during enzyme acylation. *J Biol Chem* **270:**19694–19701.

Ellman GL, Courtney KD, Andres JV and Featherstone RM (1961) A new and rapid colorimetric determination of acetylcholinesterase activity. *Biochem Pharmacol* **7:**88–95.

Harel M, Kleywegt GJ, Ravelli RBG, Silman I and Sussman JL (1995) Crystal structure of an acetylcholinesterase-fasciculin complex: Interaction of a three-fingered toxin from snake venom with its target. *Structure* **3:**1355–1366.

Harel M, Schalk I, Ehret-Sabatier L, Bouet F, Goeldner M, Hirth C, Axelsen PH, Silman I and Sussman JL (1993) Quaternary ligand binding to aromatic residues in the active-site gorge of acetylcholinesterase. *Proc Natl Acad Sci USA* **90:**9031–9035.

Hodge AS, Humphrey DR and Rosenberry TL (1992) Ambenonium is a rapidly reversible noncovalent inhibitor of acetylcholinesterase with one of the highest known affinities. *Mol Pharmacol* **41:**937–942.

Incardona JP and Rosenberry TL (1996) Construction and characterization of secreted and chimeric transmembrane forms of *Drosophila* acetylcholinesterase: A large truncation of the C-terminal signal peptide does not eliminate glycoinositol phospholipid anchoring. *Mol Biol Cell* **7:**595–611.

Kozikowski AP, Thiels E, Tang X-C and Hanin I (1992) Huperzine A—A possible lead structure in the treatment of Alzheimer's disease. *Adv Med Chem* **1:**175–205.

Lockridge O (1990) Genetic variants of human serum cholinesterase influence metabolism of the muscle relaxant succinylcholine. *Pharmacol Ther* **47:**35–60.

Mallender WD, Szegletes T and Rosenberry TL (1999) Organophosphorylation of acetylcholinesterase in the presence of peripheral site ligands: Distinct effects of propidium and fasciculin. *J Biol Chem* **274:**8491–8499.

Muramoto O, Sugishita M, Sugita H and Toyokura Y (1979) Effect of physostigmine on constructional and memory tasks in Alzheimer's disease. *Arch Neurol* **36:**501–503.

Nair HK, Lee K and Quinn DM (1993) *m*-(*N,N, N*-Trimethylammonio)trifluoroacetophenone: A femtomolar inhibitor of acetylcholinesterase. *J Am Chem Soc* **115:**9939–9941.

Pang Y-P, Quiram P, Jelacic T, Hong F and Brimijoin S (1996) Highly potent selective and low cost bis-tetrahydroaminacrine inhibitors of acetylcholinesterase. *J Biol Chem* **271:**23646–23649.

Perry EK, Perry TH, Blessed G and Tomlinson BE (1977) Necropsy evidence of central cholinergic deficits in senile dementia. *Lancet* **1:**189.

Raves ML, Harel M, Pang Y-P, Silman I, Kozikowski AP and Sussman JL (1997) Structure of acetylcholinesterase complexed with the nootropic alkaloid (−)-huperzine A. *Nat Struct Biol* **4:**57–63.

Riddles PW, Blakeley RL and Zerner B (1979) Ellman's reagent: 5, 5′-dithiobis-(2-nitrobenzoic) acid—A reexamination. *Anal Biochem* **94:**75–81.

Roberts WL, Kim BH and Rosenberry TL (1987) Differences in the glycolipid membrane anchors of bovine and human erythrocyte acetylcholinesterases. *Proc Natl Acad Sci USA* **84:**7817–7821.

Rosenberry TL (1975) Acetylcholinesterase, in *Advances in Enzymology 43* (Meister A ed) pp 103–218, John Wiley & Sons, New York.

Rosenberry TL and Bernhard SA (1972) Studies on catalysis by acetylcholinesterase: Synergistic effects of inhibitors during hydrolysis of acetic acid esters. *Biochemistry* **11:**4308–4321.

Rosenberry TL, Rabl CR and Neumann E (1996) Binding of the neurotoxin fasciculin 2 to the acetylcholinesterase peripheral site drastically reduces the association and dissociation rate constants for *N*-methylacridinium binding to the active site. *Biochemistry* **35:**685–690.

Rosenberry TL and Scoggin DM (1984) Structure of human erythrocyte acetylcholinesterase. Characterization of intersubunit disulfide bonding and detergent interaction. *J Biol Chem* **259:**5643–5652.

Sussman JL, Harel M, Frolow F, Oefner C, Goldman A, Toker L and Silman I (1991) Atomic structure of acetylcholinesterase from *Torpedo californica*: A prototypic acetylcholine-binding protein. *Science (Wash DC)* **253:**872–879.

Szegletes T, Mallender WD and Rosenberry TL (1998) Nonequilibrium analysis alters the mechanistic interpretation of inhibition of acetylcholinesterase by peripheral site ligands. *Biochemistry* **37:**4206–4216.

Szegletes T, Mallender WD, Thomas PJ and Rosenberry TL (1999) Substrate binding to the peripheral site of acetylcholinesterase initiates enzymatic catalysis. Substrate inhibition arises as a secondary effect. *Biochemistry* **38:**122–133.

Taylor P and Lappi S (1975) Interaction of fluorescence probes with acetylcholinesterase: The site and specificity of propidium binding. *Biochemistry* **14:**1989–1997.

Whitehouse PJ, Price DL, Clark AW, Coyle JT and DeLong MR (1981) Alzheimer disease: Evidence for selective loss of cholinergic neurons in the nucleus basalis. *Ann Neurol* **10:**122–126.

Send reprint requests to: Terrone L. Rosenberry, Department of Pharmacology, Mayo Clinic Jacksonville, 4500 San Pablo Rd., Jacksonville, FL 32224. E-mail: rosenb@mayo.edu